Title

Hydrogen sulfide induces Ca^{2+} release from intracellular Ca^{2+} stores and stimulates lactate production in spinal cord astrocytes.

Takeshi Nii, Ryota Eguchi, Ken-ichi Otsuguro[1]

[1]Laboratory of Pharmacology, Department of Basic Veterinary Sciences, Faculty of Veterinary Medicine, Hokkaido University, Kita 18, Nishi 9, Kita-ku, Sapporo 060-0818, Japan

Corresponding author: Ken-ichi Otsuguro

Tel/Fax: +81-11-706-5220; E-mail: otsuguro@vetmed.hokudai.ac.jp

ORCID number: 0000-0002-2481-5592

Abstract

Hydrogen sulfide (H_2S) is a well-known inhibitor of the mitochondrial electron transport chain (ETC). H_2S also increases intracellular Ca^{2+} levels in astrocytes, which are glial cells and that supply lactate as an energy substrate to neurons. Here, we examined the relationship between H_2S-induced metabolic changes and Ca^{2+} responses in spinal cord astrocytes. Na_2S (150 μM), an H_2S donor, increased the intracellular Ca^{2+} concentration, which was inhibited by an ETC inhibitor and an uncoupler of mitochondrial oxidative phosphorylation. Na_2S also increased the accumulation of extracellular lactate. Na_2S alone did not change intracellular ATP content, but decreased it when glycolysis was inhibited. The Na_2S-induced Ca^{2+} increase and accumulation of extracellular lactate were inhibited by emetine, an inhibitor of translocon complex, which mediates Ca^{2+} leak from the endoplasmic reticulum (ER). Furthermore, an inhibitor of the Ca^{2+}-sensitive NADH shuttle decreased Na_2S-mediated accumulation of lactate. We conclude that inhibition of the mitochondrial ETC by H_2S induces Ca^{2+} release from mitochondria and the ER in spinal cord astrocytes, which increases lactate production. H_2S may promote glycolysis by activating the Ca^{2+}-sensitive NADH shuttle and facilitating the supply of lactate from astrocytes to neurons.

Keywords: hydrogen sulfide, ATP, lactate, calcium, astrocytes

1. Introduction

Hydrogen sulfide (H_2S), which is a gaseous substance and smells like rotten eggs, inhibits the electron transport chain (ETC) in mitochondria at high concentrations (Cooper and Brown, 2008). Despite this toxicity, H_2S is endogenously produced in the central nervous system (CNS). The physiological concentration of H_2S in the brain is reported to be < 166 μM (Baskar and Bian, 2011). In the CNS, H_2S is produced mainly by astrocytes which is one of the glial cells (Lee et al., 2009). In hippocampal astrocytes, H_2S increases intracellular Ca^{2+} concentration ($[Ca^{2+}]_i$) mainly by activating Ca^{2+} channels on the cell membrane through the post-translational modification of protein cysteine residues (Kimura et al., 2013; Nagai et al., 2004). Our previous study has shown that H_2S increases $[Ca^{2+}]_i$ mainly by Ca^{2+} release from the endoplasmic reticulum (ER) in spinal cord astrocytes (Nii et al., 2021). However, the depletion of Ca^{2+} content in the ER did not completely suppress H_2S-induced $[Ca^{2+}]_i$ increase. Therefore, it is presumed that H_2S acts on other Ca^{2+} stores including mitochondria.

H_2S has various effects on metabolism in mitochondria depending on its concentration (Panagaki et al., 2019). Changes in mitochondrial respiration affect $[Ca^{2+}]_i$ by influencing the mitochondrial membrane potential (Zhao et al., 2013) or the concentrations of bioactive substances including ATP, which regulates the activity of Ca^{2+} leak channels on the ER membrane (Walsh et al., 2009). However, the relationship between metabolic changes induced by H_2S and changes in $[Ca^{2+}]_i$ is poorly understood.

H_2S induces not only metabolic changes in mitochondria but also promotes glycolysis and lactate production (Lee et al., 2017). Ca^{2+} is a key regulator of glycolysis. Various carriers that shuttle substances such

as NADH through the inner mitochondrial membranes are regulated by Ca^{2+} (Gellerich et al., 2010). Among these carriers, aspartate-glutamate carriers enhance glycolysis by preventing the accumulation of cytoplasmic NADH (Wang et al., 2016). In addition, the Ca^{2+}-calmodulin complex is an upstream regulator of glucose uptake and the glycolytic pathway (Herzig and Shaw, 2018).

Although lactate was originally considered as a waste product of glycolysis, this concept was changed by the discovery of a cell-to-cell lactate shuttle (Gladden, 2004). A lactate gradient from astrocytes to neurons exists in the CNS (Mächler et al., 2016), and lactate is shuttled from astrocytes to neurons as an energy substrate (Alberini et al., 2018). Recent studies indicate that lactate is an important signal for neurotransmission and memory processing (Abrantes et al., 2019; Dienel, 2019). Furthermore, the administration of lactate has neuroprotective roles after ischemia (Berthet et al., 2009).

In this study, to investigate the relationship between astrocytic metabolic changes induced by H_2S and changes in $[Ca^{2+}]_i$, we performed Ca^{2+} imaging and measured the amount of intracellular ATP and extracellular lactate. We demonstrate that H_2S increases $[Ca^{2+}]_i$ by inhibiting mitochondrial respiration and enhancing lactate production. We also show that H_2S promotes glycolysis by activating Ca^{2+}-sensitive mitochondrial carriers.

2. Materials and Methods

2.1. Reagents

Na_2S and *O*,*O*'-Bis(2-aminophenyl)ethyleneglycol-*N*,*N*,*N*',*N*'-tetraacetic acid, tetraacetoxymethyl ester (BAPTA-AM) solution was purchased from Dojindo (Kumamoto, Japan). Iodoacetic acid sodium salt (IA) and sodium pyruvate were purchased from Nacalai Tesque (Kyoto, Japan). Rotenone, *N*-(6-aminohexyl)-5-chloro-1-naphthalenesulfonamide hydrochloride (W7), and glutamic-pyruvic transaminase (GPT) were purchased from Sigma-Aldrich (St.Louis, MO, USA). L(+)-Glutamine, emetine dihydrochloride, and (aminooxy)acetic acid hemihydrochloride (AOAA) were purchased from FUJIFILM Wako Pure Chemicals Industries (Osaka, Japan). Lactate dehydrogenase was purchased from TOYOBO (Osaka, Japan). β-NAD^+ was purchased from Oriental Yeast Co., Ltd (Tokyo, Japan). Cyanide 4-trifluoromethoxyphenylhydrazone (FCCP) was purchased from Fluka (Buchs, Switzerland).

2.2. Animals

Wistar rats were obtained from Clea Japan (Tokyo, Japan). The animals had *ad libitum* access to food and tap water, and were maintained in a temperature-controlled environment on a 12:12 h light/dark cycle. Male and female pups aged 0−3 days were used for experiments. All animal care and experimental protocols were approved by the Committee on Animal Experimentation, Graduate School of Veterinary Medicine, Hokkaido University (No. 19-0009).

2.3. Cell culture

Cultured astrocytes from spinal cord were obtained from Wistar rats. Neonatal rats were killed by decapitation and the isolated spinal cord was minced with scissors in divalent cation-free Hanks' balanced salt solution. Following digestion with papain (10 U/ml) and DNase (0.1 mg/ml) at room temperature for 20 min, tissues were mechanically dissociated with a Pasteur pipette in culture medium. The culture medium was Dulbecco's modified Eagle Medium (DMEM)/Ham's-F12 containing 10% fetal bovine serum, 100 U/ml penicillin, and 0.1 mg/ml of streptomycin. The cell suspension was transferred to a poly-L-lysine-coated T75 flask, and the medium was replaced after 1−2 h. Cells were cultured in a humidified environment containing 5% CO_2 at 37°C and the culture medium was replaced every 2 or 3 days. When cells reached 80 − 90% confluence, flasks were shaken vigorously at 250 rpm for at least 12 h to remove nonadherent cells. The remaining astrocytes were trypsinized and seeded in poly-L-lysine-coated T25 flasks or cover glasses (Φ15). Almost all cells were positive for the astrocyte marker glial fibrillary acidic protein (Eguchi et al., 2015).

The cells were seeded at a density of 2.5×10^4 cells/cm^2 in T25 flasks. Once the cells reached confluence, they were plated at a density of 5×10^3 cells/cm^2 for measurement of ATP or 9×10^4 cells/cm^2 for measurement of lactate on 12-well plates and were cultured overnight. The cells were then washed with artificial cerebrospinal fluid (ACSF; 143 mM NaCl, 3.5 mM KCl, 1.25 mM $CaCl_2$, 1.2 mM $MgCl_2$, 25 mM HEPES, and 0.5 mM glucose, pH 7.3 with NaOH) and incubated for 1 h at 37°C in ACSF which contained 1 mM sodium pyruvate and 2 mM glutamine before Na_2S (at a final concentration of 1.5–150 μM) was added.

2.4. Measurement of extracellular lactate

Extracellular lactate concentration in culture media was determined using an established assay (Schmidt, 2009). Media samples (20 µl) were diluted with 160 µl purified water in wells of a micro plate and mixed with 180 µl reaction mixture (5.6 mM NAD^+, 19.9 U/ml lactate dehydrogenase, and 1.94 U/ml glutamic-pyruvic transaminase in 250 mM sodium glutamate buffer, pH 8.9 with NaOH). After incubation for 90 min in a humidified atmosphere at 37°C, the absorbance of the NADH generated from lactate was measured at 340 nm using a microplate reader (SH-9000; Corona Electric, Hitachinaka, Japan). Media samples containing no lactate were used as blanks. The remaining cells were suspended in 0.1 N NaOH and sonicated. The protein content of cell lysates was measured using the Quick Start protein assay (Bio-Rad, Hercules, CA, USA). The amount of lactate was expressed as the extracellular amount per milligram of protein in cell lysates (nmol/mg protein).

2.5. Measurement of intracellular ATP

The medium was aspirated, and cells were washed twice with ACSF and then suspended in boiling water (1 ml/well) by repeated pipetting (Yang et al., 2002). The cell suspension was then centrifuged (12,000x*g* at 4°C for 5 min), and 20 µl supernatant was used as a sample. The ATP concentration in the samples was measured with the luciferin-luciferase technique using the ATP Determination kit (Invitrogen, Carlsbad, CA, USA) and a microplate reader.

2.6. Calcium imaging

Cells were seeded on cover glasses at a density of 5×10^3 cells/cm^2 and cultured for 9−17 days. The cells were then washed with ACSF and loaded with 1 μM fura-2 acetoxymethyl ester (Dojindo) and 0.002% (v/v) Cremophor EL in ACSF for 60 min at 25°C. Fura-2 fluorescence was measured using an inverted microscope (Diaphot 300, Nikon, Tokyo, Japan) with a fluorescence ratio imaging system (ORCA-ER; Hamamatsu Photonics, Shizuoka, Japan). Cells were continuously superfused with ACSF and illuminated at 340 and 380 nm for 111 ms at 2 s intervals. The respective fluorescence signals (F_{340} and F_{380}) were detected at 500 nm. The ratio of F_{340} and F_{380} (R) was analyzed using Aquacosmos 2.6 software (Hamamatsu Photonics). The intracellular calcium concentration ($[Ca^{2+}]_i$) was calculated using the following equation : $[Ca^{2+}]_i = K_D\beta \times (R—R_{min}) / (R_{max}-R)$ (Grynkiewicz et al., 1985). The dissociation constant of fura-2 and Ca^{2+} (K_D), the ratio of F_{380} at saturating Ca^{2+} to F_{380} at zero Ca^{2+} (β), and the minimum (R_{min}) and maximum (R_{max}) of the fluorescence ratio (F_{340}/F_{380}) were calculated using a calcium calibration buffer kit (Invitrogen).

Basal $[Ca^{2+}]_i$ was determined at a single time point just before application of compounds. Peak $[Ca^{2+}]_i$ was determined from a maximum fluorescence point during application of drugs. The peak amplitude was calculated as the difference between peak $[Ca^{2+}]_i$ and basal $[Ca^{2+}]_i$. The area under the curve (AUC, nM*min) during the application of compounds was calculated using Excel 2016 (Microsoft, Redmond, WA, USA). An AUC value of 0 or less was treated as 0.

2.7. Statistical analysis

Data are expressed as means ± standard errors of the means (S.E.M.). Statistical comparisons between two groups were assessed using Student's *t*-tests, and analyses of variance followed by Dunnett's test or Tukey's test was used for multiple comparisons. A *P*-value <0.05 was considered significant. Ekuseru–Toukei 2008 statistical software (Social Survey Research Information Co., Ltd., Tokyo, Japan) was used for all statistical analyses.

3. Results

3.1. H_2S increases $[Ca^{2+}]_i$ by inhibiting the mitochondrial ETC.

H_2S is reported to inhibit the mitochondrial ETC (Cooper and Brown, 2008). Inhibition of the ETC induces depolarization of the mitochondrial inner membrane (Barrientos and Moraes, 1999; Eghbal et al., 2004), which triggers Ca^{2+} release from mitochondria (Saotome et al., 2005; Zhao et al., 2013). Thus, we first examined whether inhibition of the ETC by H_2S alters $[Ca^{2+}]_i$ in spinal cord astrocytes. Na_2S (150 μM, 10 min), an H_2S donor, increased $[Ca^{2+}]_i$ (Fig. 1A, B) as previously reported (Nii et al., 2021). The application of rotenone (10 μM, 5 min), an inhibitor of the ETC (Wilhelm and Hirrlinger, 2011), also increased $[Ca^{2+}]_i$. Furthermore, Na_2S-induced increases in $[Ca^{2+}]_i$ was reduced after pretreatment of rotenone, but did not disappear completely. Extending the application time of rotenone to 10 min had the same result (Fig. S1). In our previous study, the depletion of Ca^{2+} content in the ER by thapsigargin suppressed H_2S-induced $[Ca^{2+}]_i$ increase (Nii et al., 2021). Similarly, pretreatment of thapsigargin (1 μM, 10 min) suppressed rotenone-induced $[Ca^{2+}]_i$ increase (Fig. S2).These results suggest that H_2S increases $[Ca^{2+}]_i$ by inhibiting the ETC, and which is mediated mainly through Ca^{2+} release from the ER.

Next, we examined whether H_2S induces Ca^{2+} release from mitochondria. FCCP, an uncoupling protonophore, releases Ca^{2+} from mitochondria by the rapid depolarization of mitochondrial membrane potential, which reduces the mitochondrial Ca^{2+} content (Saotome et al., 2005). Application of FCCP (5 μM, 5 min) increased $[Ca^{2+}]_i$ in the spinal cord astrocytes, and this response was reduced following pretreatment with Na_2S

(150 μM, 5 min) (Fig. 1C, D). This result suggests that H_2S reduces Ca^{2+} content in the mitochondria. Although the peak amplitude of Na_2S-induced $[Ca^{2+}]_i$ response did not changed, after pretreatment of FCCP, the AUC value decreased (Fig. 1E, F). The reduction in the Na_2S-induced $[Ca^{2+}]_i$ response by FCCP appeared 1 min after the application of Na_2S (Fig. S3). These results suggest that H_2S releases Ca^{2+} from mitochondria, but its amount is small relative to the overall H_2S-induced $[Ca^{2+}]_i$ response.

3.2. H_2S promotes glycolysis and inhibits oxidative phosphorylation.

Inhibition of the mitochondrial ETC induces a compensatory increase in glycolysis (Hou et al., 2018), which increases lactate production and release from cells. We examined the effect of H_2S on glycolysis in cultured spinal cord astrocytes using extracellular lactate accumulation as a measure of increased glycolysis. Application of Na_2S (150 μM, 30 min) increased the amount of extracellular lactate (Fig. 2A). A significant increase in extracellular lactate was observed 30 min, but not 10 or 60 min, after application of 150 μM Na_2S (Fig. 2B). Furthermore, application of IA (1 mM, 30 min), an inhibitor of glycolysis (Schmidt, 2009), alone did not affect the amount of extracellular lactate. In the presence of IA, Na_2S (150 μM) did not increase the amount of extracellular lactate (Fig. 2C). These results suggest that H_2S promotes the production of new lactate.

We next examined whether H_2S affects ATP synthesis (Fig. 2D). The application of Na_2S (150 μM, 10 min) did not change intracellular ATP content. IA (1 mM, 10 min) also had no significant effect on the ATP content. On the other hand, the co-application of IA and Na_2S significantly decreased the ATP content. These results

suggest that H_2S inhibits ATP synthesis by oxidative phosphorylation, but total ATP content is maintained for at least 10 min by a compensatory increase in glycolysis.

We then examined whether increased glycolysis contributes to the H_2S-induced increase in $[Ca^{2+}]_i$ in spinal cord astrocytes. The application of IA (1 mM, 10 min) increased $[Ca^{2+}]_i$, and enhanced the Na_2S (150 μM)-induced $[Ca^{2+}]_i$ increase (Fig. S4). This result suggests that the H_2S-induced $[Ca^{2+}]_i$ response is not mediated by increased glycolysis.

3.3. H_2S-induced Ca^{2+} release through the translocon complex promotes glycolysis.

As FCCP did not completely inhibit H_2S-induced increase in $[Ca^{2+}]_i$ (Fig. 1C), H_2S may increase $[Ca^{2+}]_i$ with a different mechanism from the Ca^{2+} release from mitochondria. In our previous study, H_2S increases $[Ca^{2+}]_i$ mainly by Ca^{2+} release from the ER in spinal cord astrocytes (Nii et al., 2021). The inhibition of oxidative phosphorylation decreases the ATP content in the ER (Yong et al., 2019). In the ER, ATP regulates the translocon complex, which is the main gate for the translocation of nascent peptides into the ER (Hamman et al., 1998). In addition, the translocon complex functions as a Ca^{2+} leak channel when ATP is decreased in the ER (Klein et al., 2018). The Ca^{2+} leak through translocon complex on the ER membrane is inhibited by application of 40 μM emetine for 1 h (Amer et al., 2009). Preincubation of cells with emetine (40 μM, 1 h) significantly reduced basal $[Ca^{2+}]_i$ (control: 67.95 ± 2.61 nM, vs. emetine: 48.69 ± 2.32 nM, $P < 0.01$ unpaired Student's t-test, n = 93 cells from 3 cultures) and the $[Ca^{2+}]_i$ response to Na_2S (150 μM, 10 min) (Fig. 3A, B). The

reduction in Na_2S-induced $[Ca^{2+}]_i$ response by emetine appeared 1 min after the application of Na_2S (Fig. S5). These results suggest that H_2S induces Ca^{2+} release from the ER through the translocon complex.

Ca^{2+} leak through the translocon complex promotes glycolysis (Klein et al., 2018). Therefore, we examined whether H_2S-induced changes in $[Ca^{2+}]_i$ affect glycolysis. Incubation of cells with BAPTA-AM alone (50 μM, 30 min), a membrane permeable Ca^{2+} chelator, did not affect the amount of extracellular lactate accumulation (Fig. 3C). Preincubation of BAPTA-AM abolished Na_2S-mediated increase in lactate accumulation. Furthermore, to investigate whether the H_2S-induced Ca^{2+} release through the translocon complex is involved in H_2S-mediated increase in glycolysis, we measured extracellular lactate in the presence of emetine (Fig. 3D). Incubation of cells with emetine alone (40 μM, 1 h) did not affect the amount of extracellular lactate accumulation. Preincubation of cells with emetine (40 μM, 1 h) prior to treatment with Na_2S (150 μM, 30 min) suppressed Na_2S-mediated increase in lactate accumulation. These results suggest that H_2S-induced Ca^{2+} release through the translocon complex promotes glycolysis.

Next, we investigated the mechanism by which the H_2S-mediated Ca^{2+} response promotes glycolysis. To maintain synthesis of ATP during enhanced glycolysis, a mechanism to prevent excessive increases in cytoplasmic NADH needs to exist (Wang et al., 2016). The malate-aspartate shuttle (MAS), which is involved in transport of NADH through the inner mitochondrial membrane, is sensitive to extramitochondrial Ca^{2+} in astrocytes (McKenna et al., 2006). We examined whether MAS is involved in H_2S-mediated enhancement of glycolysis. The MAS inhibitor AOAA (5 mM, 20 min) alone did not affect the amount of extracellular lactate accumulation (Fig. 3E), but suppressed the Na_2S (150 μM)-evoked increase in extracellular lactate. These

results suggest that the transporting activity of MAS is not high under basal conditions but contributes to the promotion of glycolysis by H_2S.

The translocon complex-mediated Ca^{2+} release is reported to phosphorylate AMP-activated protein kinase (AMPK) (Klein et al., 2018), which is also activated by calcium/calmodulin-dependent pathway (Racioppi and Means, 2012). We next examined whether calmodulin is involved in H_2S-mediated enhancement of glycolysis. Astrocytes were preincubated with W7 (50 μM, 30 min), a calmodulin inhibitor, followed by incubation with or without Na_2S (150 μM), and then extracellular lactate accumulation was measured. W7 alone tended to increase the amount of extracellular lactate, and W7 inhibited Na_2S-induced lactate accumulation (Fig. 3F).

4. Discussion

In this study, we demonstrated that H_2S increases $[Ca^{2+}]_i$ and lactate release from spinal cord astrocytes. In addition to Ca^{2+} release from mitochondria, mediated by inhibition of the ETC, H_2S releases Ca^{2+} from the ER through the translocon complex. It was also shown that the H_2S-mediated Ca^{2+} release stimulates a compensatory increase in glycolysis in spinal cord astrocytes (Fig. S6).

Na_2S (150 μM) increased $[Ca^{2+}]_i$ in cultured spinal cord astrocytes. H_2S at high concentrations (>20 μM) inhibits the mitochondrial ETC (Cooper and Brown, 2008). In water, Na_2S (150 μM) produces a concentration of H_2S of approximately 40 μM because the pKa value of H_2S is 6.98 (at 25°C) (Filipovic et al., 2018). Therefore, in this study, it is suggested that H_2S suppresses mitochondrial ETC when Na_2S (150 μM) increases $[Ca^{2+}]_i$. Furthermore, the H_2S-induced Ca^{2+} response was significantly suppressed by rotenone, and rotenone also increased $[Ca^{2+}]_i$. Rotenone is an inhibitor of ETC (Hou et al., 2018). These results suggest that inhibition of the ETC by H_2S triggers the Ca^{2+} response. FCCP also inhibited the H_2S-induced Ca^{2+} response. FCCP releases Ca^{2+} from mitochondria by depolarizing the mitochondrial membrane potential (Saotome et al., 2005), which is also mediated via the inhibition of ETC (Barrientos and Moraes, 1999). We suggest that H_2S also depolarizes the mitochondrial membrane potential, which is consistent with previous finding (Eghbal et al., 2004). Taken together, our results and published literature indicate that H_2S releases Ca^{2+} from mitochondria in spinal cord astrocytes.

We also found that the H_2S-induced Ca^{2+} response was inhibited by emetine, which inhibits Ca^{2+} leak from the ER through the translocon complex (Amer et al., 2009). This complex functions as a Ca^{2+} leak channel when ATP content in the ER decreases (Klein et al., 2018). A recent study indicated that ATP in the ER originates from mitochondria (Yong et al., 2019). Moreover, considering that H_2S inhibits mitochondrial respiration, we suggest that inhibition of ATP synthesis in mitochondria by H_2S induces Ca^{2+} release from the ER through the translocon complex.

H_2S regulates protein function by covalently modifying cysteine residues, process known as *S*-sulfhydration (Mustafa et al., 2009). In hippocampal astrocytes, H_2S increases $[Ca^{2+}]_i$ mainly by Ca^{2+} influx through *S*-sulfhydrated transient receptor potential (TRP) A1 channels (Kimura et al., 2013; Nagai et al., 2004). In these previous studies, removal of extracellular Ca^{2+} does not completely inhibit the H_2S-induced $[Ca^{2+}]_i$ increase, suggesting that a small amount of Ca^{2+} release from intracellular Ca^{2+} stores is involved in H_2S. In spinal cord astrocytes, our previous study demonstrated that in spinal cord astrocytes H_2S increases $[Ca^{2+}]_i$ mainly by Ca^{2+} release from the ER in a *S*-sulfhydration-independent manner (Nii et al., 2021). In addition, the present study shows that the inhibitors of ETC or the translocon complex markedly suppressed H_2S-induced increase in $[Ca^{2+}]_i$. The mechanisms involved in H_2S-induced Ca^{2+} responses may vary depending on the region from which astrocytes are obtained. Further investigation is needed to reveal the H_2S-mediated astrocytic Ca^{2+} signals in the spinal cord.

Na_2S increased the amount of extracellular lactate without affecting ATP content, while it decreased ATP content during inhibition of glycolysis by IA. These results indicate that H_2S inhibits ATP synthesis in

mitochondria, while increases in glycolysis keep ATP content constant. These results also support the notion that H_2S increases $[Ca^{2+}]_i$ by inhibiting of mitochondrial ETC in spinal cord astrocytes.

The H_2S-induced accumulation of extracellular lactate was inhibited by emetine. Furthermore, AOAA, a MAS inhibitor, inhibited lactate accumulation induced by H_2S. Cytoplasmic Ca^{2+} modulates intracellular respiration by increasing the activity of aspartate-glutamate carriers, which are components of MAS required for shuttling NADH. Aspartate-glutamate carriers are activated by Ca^{2+} with an $S_{0.5}$ value of 350 nM (Contreras et al., 2007). In our study, H_2S increased $[Ca^{2+}]_i$ by approximately 60 nM as an average for the entire cytoplasm, but this value appears too low to activate aspartate-glutamate carriers. The local change of concentration in Ca^{2+} concentration near the mitochondrial membrane could be higher because of the existence of high $[Ca^{2+}]_i$ nanodomains at ER−mitochondria contacts when Ca^{2+} is released from the ER (Csordás et al., 2018). The activation of MAS promotes glycolysis by preventing the accumulation of cytoplasmic NADH (Wang et al., 2016). From these findings, we suggest that H_2S-induced Ca^{2+} release from the ER through the translocon complex stimulates MAS and contributes to the promotion of glycolysis.

A previous study showed that Ca^{2+} leak through the translocon complex activates AMPK (Klein et al., 2018). AMPK is a downstream of calmodulin-mediated signaling pathway to stimulate glucose utilization (Herzig and Shaw, 2018; Racioppi and Means, 2012). However, in our study, the role of calmodulin was not clear; the calmodulin inhibitor W7 tended to increase extracellular lactate, and W7 inhibited the H_2S-induced lactate accumulation. Inhibition of calcium/calmodulin-dependent protein kinase II depolarizes the mitochondrial membrane potential in the hippocampal astrocytes (Ashpole et al., 2013). Therefore, it is possible

that inhibiting calmodulin deactivates oxidative phosphorylation in mitochondria and promotes a compensatory increase in glycolysis. Further investigation is needed to reveal whether calmodulin is involved in glycolysis enhanced by H_2S.

In conclusion, inhibition of the mitochondrial ETC by H_2S induces an increase in $[Ca^{2+}]_i$ in spinal cord astrocytes, which promotes a compensatory increase in glycolysis. Lactate, a glycolytic product, is shuttled from astrocytes to neurons as an energy substrate and signaling molecules (Alberini et al., 2018). Therefore, H_2S-induced $[Ca^{2+}]_i$ increase may facilitate the supply of lactate from astrocytes to neurons required to maintain homeostasis in the CNS.

Conflicts of interest

The authors declare that they have no conflicts of interest.

Acknowledgments

This work was supported by a Grant-in-Aid for Scientific Research from the Japan Society for the Promotion of Science (no. 19K23701).

References

Abrantes, H. de C., Briquet, M., Schmuziger, C., Restivo, L., Puyal, J., Rosenberg, N., Rocher, A.B., Offermanns, S., Chatton, J.Y., 2019. The lactate receptor HCAR1 modulates neuronal network activity through the activation of G_{α} and $G_{\beta\gamma}$ subunits. J. Neurosci. 39, 4422–4433. https://doi.org/10.1523/JNEUROSCI.2092-18.2019

Alberini, C.M., Cruz, E., Descalzi, G., Bessières, B., Gao, V., 2018. Astrocyte glycogen and lactate: new insights into learning and memory mechanisms. Glia 66, 1244–1262. https://doi.org/10.1002/glia.23250

Amer, M.S., Li, J., O'regan, D.J., Steele, D.S., Porter, K.E., Sivaprasadarao, A., Beech, D.J., 2009. Translocon closure to Ca^{2+} leak in proliferating vascular smooth muscle cells. Am J Physiol Hear. Circ Physiol 296, 910–916. https://doi.org/10.1152/ajpheart.00984.2008

Ashpole, N.M., Chawla, A.R., Martin, M.P., Brustovetsky, T., Brustovetsky, N., Hudmon, A., 2013. Loss of calcium/calmodulin-dependent protein kinase II activity in cortical astrocytes decreases glutamate uptake and induces neurotoxic release of ATP. J. Biol. Chem. 288, 14599–14611. https://doi.org/10.1074/jbc.M113.466235

Barrientos, A., Moraes, C.T., 1999. Titrating the effects of mitochondrial complex I impairment in the cell physiology. J. Biol. Chem. 274, 16188–16197. https://doi.org/10.1074/jbc.274.23.16188

Baskar, R., Bian, J., 2011. Hydrogen sulfide gas has cell growth regulatory role. Eur. J. Pharmacol. 656, 5–9. https://doi.org/10.1016/j.ejphar.2011.01.052

Berthet, C., Lei, H., Thevenet, J., Gruetter, R., Magistretti, P.J., 2009. Neuroprotective role of lactate after cerebral ischemia. J. Cereb. Blood Flow Metab. 29, 1780–1789. https://doi.org/10.1038/jcbfm.2009.97

Contreras, L., Gomez-Puertas, P., Iijima, M., Kobayashi, K., Saheki, T., Satrústegui, J., 2007. Ca^{2+} activation kinetics of the two aspartate-glutamate mitochondrial carriers, aralar and citrin. J. Biol. Chem. 282, 7098–7106. https://doi.org/10.1074/jbc.M610491200

Cooper, C.E., Brown, G.C., 2008. The inhibition of mitochondrial cytochrome oxidase by the gases carbon monoxide, nitric oxide, hydrogen cyanide and hydrogen sulfide: chemical mechanism and physiological significance. J. Bioenerg. Biomembr. 40, 533–539. https://doi.org/10.1007/s10863-008-9166-6

Csordás, G., Weaver, D., Hajnóczky, G., 2018. Endoplasmic reticulum–mitochondrial contactology: structure and signaling functions. Trends Cell Biol. 28, 523–540. https://doi.org/10.1016/j.tcb.2018.02.009

Dienel, G.A., 2019. Does shuttling of glycogen-derived lactate from astrocytes to neurons take place during neurotransmission and memory consolidation? J. Neurosci. Res. 97, 863–882. https://doi.org/10.1002/jnr.24387

Eghbal, M.A., Pennefather, P.S., O'Brien, P.J., 2004. H_2S cytotoxicity mechanism involves reactive oxygen species formation and mitochondrial depolarisation. Toxicology 203, 69–76. https://doi.org/10.1016/j.tox.2004.05.020

Eguchi, R., Akao, S., Otsuguro, K., Yamaguchi, S., Ito, S., 2015. Different mechanisms of extracellular adenosine accumulation by reduction of the external Ca^{2+} concentration and inhibition of adenosine metabolism in spinal astrocytes. J. Pharmacol. Sci. 128, 47–53. https://doi.org/10.1016/j.jphs.2015.04.008

Filipovic, M.R., Zivanovic, J., Alvarez, B., Banerjee, R., 2018. Chemical biology of H_2S signaling through persulfidation. Chem. Rev. 118, 1253–1337. https://doi.org/10.1021/acs.chemrev.7b00205

Gellerich, F.N., Gizatullina, Z., Trumbeckaite, S., Nguyen, H.P., Pallas, T., Arandarcikaite, O., Vielhaber, S., Seppet, E., Striggow, F., 2010. The regulation of OXPHOS by extramitochondrial calcium. Biochim. Biophys. Acta - Bioenerg. 1797, 1018–1027. https://doi.org/10.1016/j.bbabio.2010.02.005

Gladden, L.B., 2004. Lactate metabolism: a new paradigm for the third millennium. J. Physiol. 558, 5–30. https://doi.org/10.1113/jphysiol.2003.058701

Grynkiewicz, G., Poenie, M., Tsien, R.Y., 1985. A new generation of Ca^{2+} indicators with greatly improved fluorescence properties. J. Biol. Chem. 260, 3440–3450.

Hamman, B.D., Hendershot, L.M., Johnson, A.E., 1998. BiP maintains the permeability barrier of the ER membrane by sealing the lumenal end of the translocon pore before and early in translocation. Cell 92, 747–758. https://doi.org/10.1016/S0092-8674(00)81403-8

Herzig, S., Shaw, R.J., 2018. AMPK: guardian of metabolism and mitochondrial homeostasis. Nat. Rev. Mol. Cell Biol. 19, 121–135. https://doi.org/10.1038/nrm.2017.95

Hou, W.L., Yin, J., Alimujiang, M., Yu, X.Y., Ai, L.G., Bao, Y.Q., Liu, F., Jia, W.P., 2018. Inhibition of mitochondrial complex I improves glucose metabolism independently of AMPK activation. J. Cell. Mol. Med. 22, 1316–1328. https://doi.org/10.1111/jcmm.13432

Kimura, Y., Mikami, Y., Osumi, K., Tsugane, M., Oka, J., Kimura, H., 2013. Polysulfides are possible H_2S-derived signaling molecules in rat brain. FASEB J. 27, 2451–2457. https://doi.org/10.1096/fj.12-226415

Klein, M.-C., Zimmermann, K., Schorr, S., Landini, M., Klemens, P.A.W., Altensell, J., Jung, M., Krause, E., Nguyen, D., Helms, V., Rettig, J., Fecher-Trost, C., Cavalié, A., Hoth, M., Bogeski, I., Neuhaus, H.E., Zimmermann, R., Lang, S., Haferkamp, I., 2018. AXER is an ATP/ADP exchanger in the membrane of the endoplasmic reticulum. Nat. Commun. 9, 3489. https://doi.org/10.1038/s41467-018-06003-9

Lee, M., Schwab, C., Yu, S., McGeer, E., McGeer, P.L., 2009. Astrocytes produce the antiinflammatory and neuroprotective agent hydrogen sulfide. Neurobiol. Aging 30, 1523–1534. https://doi.org/10.1016/j.neurobiolaging.2009.06.001

Lee, Z.W., Teo, X.Y., Song, Z.J., Nin, D.S., Novera, W., Choo, B.A., Dymock, B.W., Moore, P.K., Huang, R.Y.J., Deng, L.W., 2017. Intracellular hyper-acidification potentiated by hydrogen sulfide mediates invasive and therapy resistant cancer cell death. Front. Pharmacol. 8, 1–10. https://doi.org/10.3389/fphar.2017.00763

Mächler, P., Wyss, M.T., Elsayed, M., Stobart, J., Gutierrez, R., Von Faber-Castell, A., Kaelin, V., Zuend, M., San Martín, A., Romero-Gómez, I., Baeza-Lehnert, F., Lengacher, S., Schneider, B.L., Aebischer, P., Magistretti, P.J., Barros, L.F., Weber, B., 2016. In vivo evidence for a lactate gradient from astrocytes to neurons. Cell Metab. 23, 94–102. https://doi.org/10.1016/j.cmet.2015.10.010

McKenna, M.C., Waagepetersen, H.S., Schousboe, A., Sonnewald, U., 2006. Neuronal and astrocytic shuttle mechanisms for cytosolic-mitochondrial transfer of reducing equivalents: current evidence and pharmacological tools. Biochem. Pharmacol. https://doi.org/10.1016/j.bcp.2005.10.011

Mustafa, A.K., Gadalla, M.M., Sen, N., Kim, S., Mu, W., Gazi, S.K., Barrow, R.K., Yang, G., Wang, R., Snyder, S.H., 2009. H_2S signals through protein S-sulfhydration. Sci. Signal. 2, ra72. https://doi.org/10.1126/scisignal.2000464

Nagai, Y., Tsugane, M., Oka, J., Kimura, H., 2004. Hydrogen sulfide induces calcium waves in astrocytes. FASEB J. 18, 557–559. https://doi.org/10.1096/fj.03-1052fje

Nii, T., Eguchi, R., Yamaguchi, S., Otsuguro, K., 2021. Hydrogen sulfide induces Ca^{2+} release from the endoplasmic reticulum and suppresses ATP-induced Ca^{2+} signaling in rat spinal cord astrocytes. Eur. J. Pharmacol 891. https://doi.org/10.1016/j.ejphar.2020.173684

Panagaki, T., Randi, E.B., Augsburger, F., Szabo, C., 2019. Overproduction of H_2S, generated by CBS, inhibits mitochondrial Complex IV and suppresses oxidative phosphorylation in down syndrome. Proc. Natl. Acad. Sci. U. S. A. 116, 18769–18771. https://doi.org/10.1073/pnas.1911895116

Racioppi, L., Means, A.R., 2012. Calcium/calmodulin-dependent protein kinase kinase 2: roles in signaling and pathophysiology. J. Biol. Chem. 287, 31658–31665. https://doi.org/10.1074/jbc.R112.356485

Salter, M.W., Hicks, J.L., 1994. ATP-evoked increases in intracellular calcium in neurons and glia from the dorsal spinal cord. J. Neurosci. 14, 1563–575. https://doi.org/10.1523/JNEUROSCI.14-03-01563.1994

Saotome, M., Katoh, H., Satoh, H., Nagasaka, S., Yoshihara, S., Terada, H., Hayashi, H., 2005. Mitochondrial membrane potential modulates regulation of mitochondrial Ca^{2+} in rat ventricular myocytes. Am. J. Physiol. Circ. Physiol. 288, H1820–H1828. https://doi.org/10.1152/ajpheart.00589.2004

Schmidt, M.M., 2009. Differential effects of iodoacetamide and iodoacetate on glycolysis and glutathione metabolism of cultured astrocytes. Front. Neuroenergetics 1. https://doi.org/10.3389/neuro.14.001.2009

Walsh, C., Barrow, S., Voronina, S., Chvanov, M., Petersen, O.H., Tepikin, A., 2009. Modulation of calcium signalling by mitochondria. Biochim. Biophys. Acta - Bioenerg. 1787, 1374–1382. https://doi.org/10.1016/j.bbabio.2009.01.007

Wang, C., Chen, H., Zhang, M., Zhang, J., Wei, X., Ying, W., 2016. Malate-aspartate shuttle inhibitor aminooxyacetic acid leads to decreased intracellular ATP levels and altered cell cycle of C6 glioma cells by inhibiting glycolysis. Cancer Lett. 378, 1–7. https://doi.org/10.1016/j.canlet.2016.05.001

Wilhelm, F., Hirrlinger, J., 2011. The NAD^+/NADH redox state in astrocytes: independent control of the NAD^+ and NADH content. J. Neurosci. Res. 89, 1956–1964. https://doi.org/10.1002/jnr.22638

Yang, N.-C., Ho, W.-M., Chen, Y.-H., Hu, M.-L., 2002. A convenient one-step extraction of cellular ATP using boiling water for the luciferin–luciferase assay of ATP. Anal. Biochem. 306, 323–327. https://doi.org/10.1006/abio.2002.5698

Yong, J., Bischof, H., Burgstaller, S., Siirin, M., Murphy, A., Malli, R., Kaufman, R.J., 2019. Mitochondria supply ATP to the ER through a mechanism antagonized by cytosolic Ca^{2+}. eLife 8. https://doi.org/10.7554/eLife.49682

Zhao, Z., Gordan, R., Wen, H., Fefelova, N., Zang, W.-J., Xie, L.-H., 2013. Modulation of intracellular calcium waves and triggered activities by mitochondrial Ca flux in mouse cardiomyocytes. PLoS One 8, e80574. https://doi.org/10.1371/journal.pone.0080574

Figure legends

Fig. 1 Inhibition of the mitochondrial ETC by H_2S induces $[Ca^{2+}]_i$ elevation in spinal cord astrocytes.

(A, B) Representative intracellular Ca^{2+} concentration ($[Ca^{2+}]_i$) response to Na_2S (150 μM) in the absence or presence of rotenone (10 μM, A). Rotenone (Rot) was added to cells 5 min before application of Na_2S. Peak amplitudes and area under the curve (AUC) of the $[Ca^{2+}]_i$ increase induced by Na_2S are summarized (B). n = 73−80 cells from three cultures. (C, D) Representative $[Ca^{2+}]_i$ response to cyanide 4-trifluoromethoxyphenylhydrazone (FCCP; 5 μM) in the absence or presence of Na_2S (150 μM, C). Cells were treated with Na_2S for 5 min before application of FCCP. Peak amplitudes and AUC of the $[Ca^{2+}]_i$ increase induced by FCCP are summarized (D). n = 101−105 cells from three cultures. (E, F) Representative $[Ca^{2+}]_i$ response to Na_2S (150 μM) in the absence or presence of FCCP (5 μM, E). Cells were treated with FCCP for 5 min before application of Na_2S. Peak amplitudes and AUC of the $[Ca^{2+}]_i$ increase induced by Na_2S are summarized (F). n = 90−103 cells from three cultures. Data are presented as means ± S.E.M. $^{**}P < 0.01$ by unpaired Student's t-test.

Fig. 2 H_2S enhances glycolysis in spinal cord astrocytes.

(A) Lactate content in the extracellular medium from spinal cord astrocytes incubated for 30 min with Na_2S (0−150 μM). n = 5. (B) Lactate content in extracellular medium from spinal cord astrocytes incubated for up to 60 min with or without Na_2S (150 μM). n = 6. (C) Lactate content in extracellular medium from spinal cord astrocytes incubated with or without Na_2S (150 μM) and/or IA (1 mM) for 30 min. n = 5. (D) Intracellular ATP

content of spinal cord astrocytes incubated with or without Na_2S (150 μM) in the presence or absence of iodoacetic acid (IA; 1 mM) for 10 min. n = 4. Data are presented as means ± S.E.M. $^{\#}P < 0.05$, $^{\#\#}P < 0.01$ by Dunnett's test (A, D) or Tukey's test (C) for comparison of multiple groups. $^{**}P < 0.01$ by unpaired Student's t-test for comparison of two groups (B).

Fig. 3 H_2S-induced Ca^{2+} release through the translocon complex promotes glycolysis.

(A, B) Representative $[Ca^{2+}]_i$ response to Na_2S (150 μM) after incubation with or without emetine (40 μM for 60 min, A) Peak amplitudes and AUC of the $[Ca^{2+}]_i$ increase induced by Na_2S are summarized (B). n = 93 cells from three cultures. (C) Lactate content in extracellular medium from spinal cord astrocytes incubated with or without Na_2S (150 μM) for 30 min in the presence or absence of BAPTA-AM (50 μM). BAPTA-AM was applied 30 min before the start of the experiment. n = 6. (D) Lactate content in extracellular medium from spinal cord astrocytes incubated with or without Na_2S (150 μM) for 30 min in the presence or absence of emetine (40 μM). Emetine was applied 60 min before the start of the experiment. n = 6. (E) Lactate content in extracellular medium from spinal cord astrocytes incubated with or without (aminooxy)acetic acid hemihydrochloride (AOAA; 1 mM) for 20 min in the presence or absence of Na_2S (150 μM). Na_2S was applied 10 min before the start of the experiment. n = 5. (F) Lactate content in extracellular medium from spinal cord astrocytes incubated with or without Na_2S (150 μM) for 30 min in the presence or absence of W7 (50 μM). W7 was applied 30 min before the start of the experiment. n = 5. Data are presented as means ± S.E.M. $^{**}P < 0.01$ by unpaired Student's t-test or $^{\#\#}P < 0.01$, $^{\#}P < 0.05$ by Tukey's test.

Fig. 1

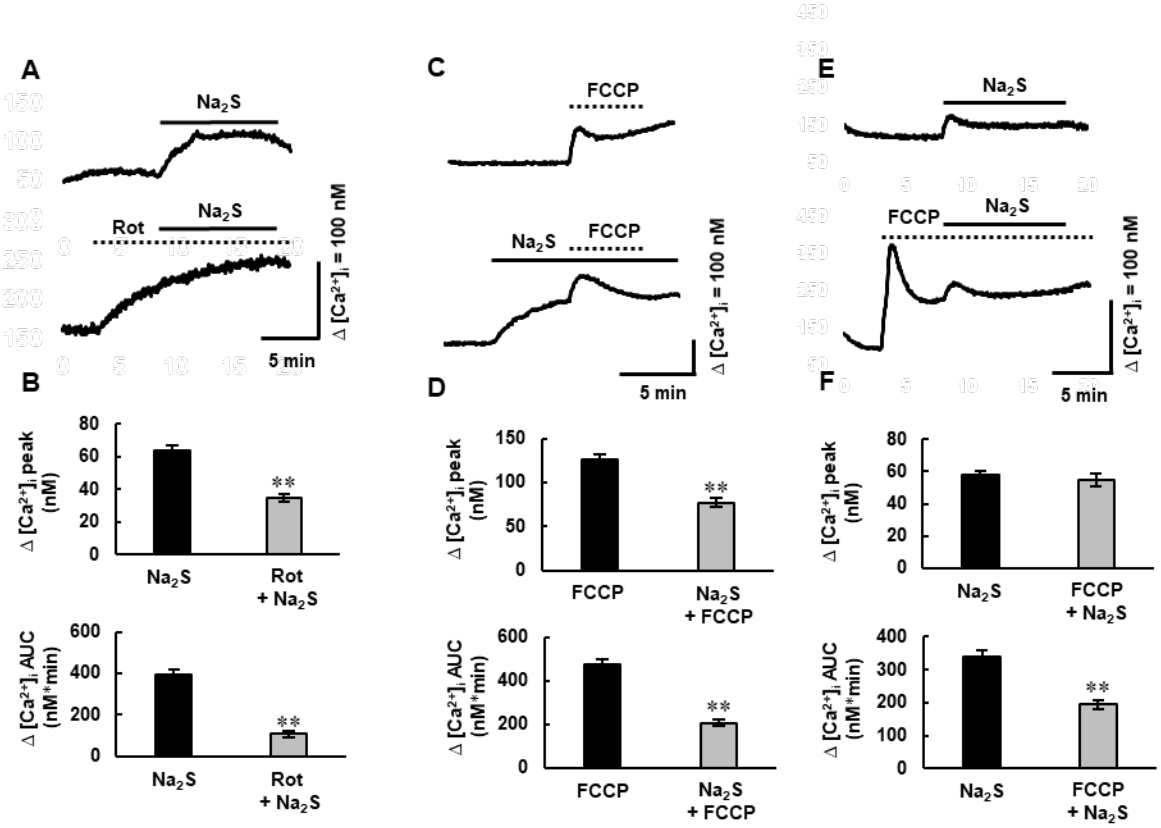
A
Na2S
Rot
Na2S
Δ [Ca2+]i = 100 nM
5 min
B
Δ [Ca2+]i peak (nM)
Na2S
Rot + Na2S
Δ [Ca2+]i AUC (nM*min)
Na2S
Rot + Na2S
C
FCCP
Na2S
FCCP
Δ [Ca2+]i = 100 nM
5 min
D
Δ [Ca2+]i peak (nM)
FCCP
Na2S + FCCP
Δ [Ca2+]i AUC (nM*min)
FCCP
Na2S + FCCP
E
Na2S
FCCP
Na2S
Δ [Ca2+]i = 100 nM
5 min
F
Δ [Ca2+]i peak (nM)
Na2S
FCCP + Na2S
Δ [Ca2+]i AUC (nM*min)
Na2S
FCCP + Na2S

Fig. 2

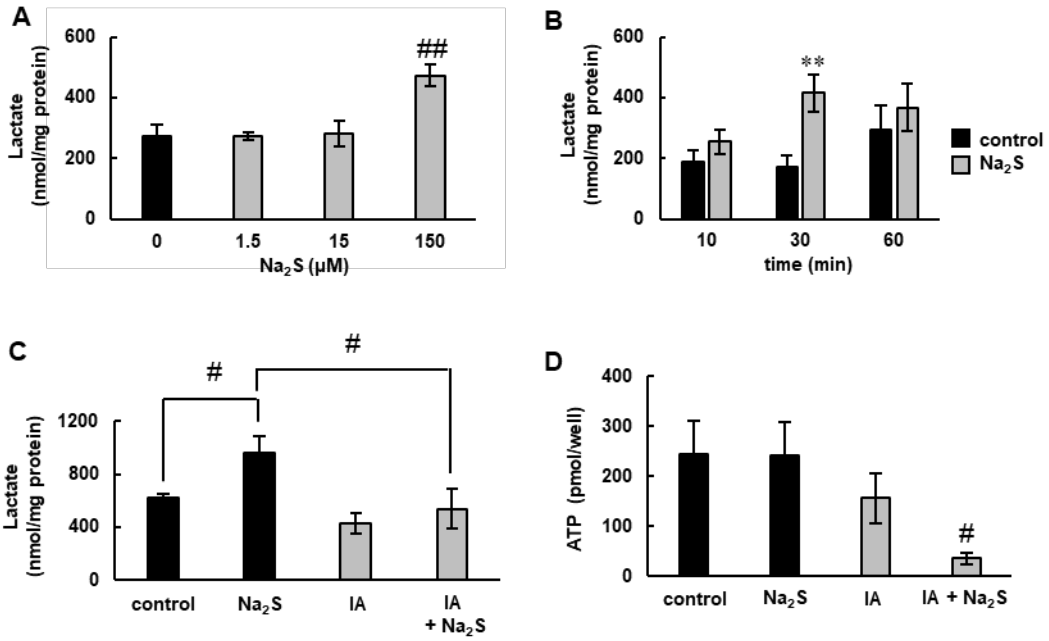
A
Lactate (nmol/mg protein)
600
400
200
0
##
0
1.5
15
150
Na2S (μM)
B
Lactate (nmol/mg protein)
600
400
200
0
**
10
30
60
time (min)
control
Na2S
C
Lactate (nmol/mg protein)
1200
800
400
0
#
#
control
Na2S
IA
IA + Na2S
D
ATP (pmol/well)
400
300
200
100
0
#
control
Na2S
IA
IA + Na2S

Fig. 3

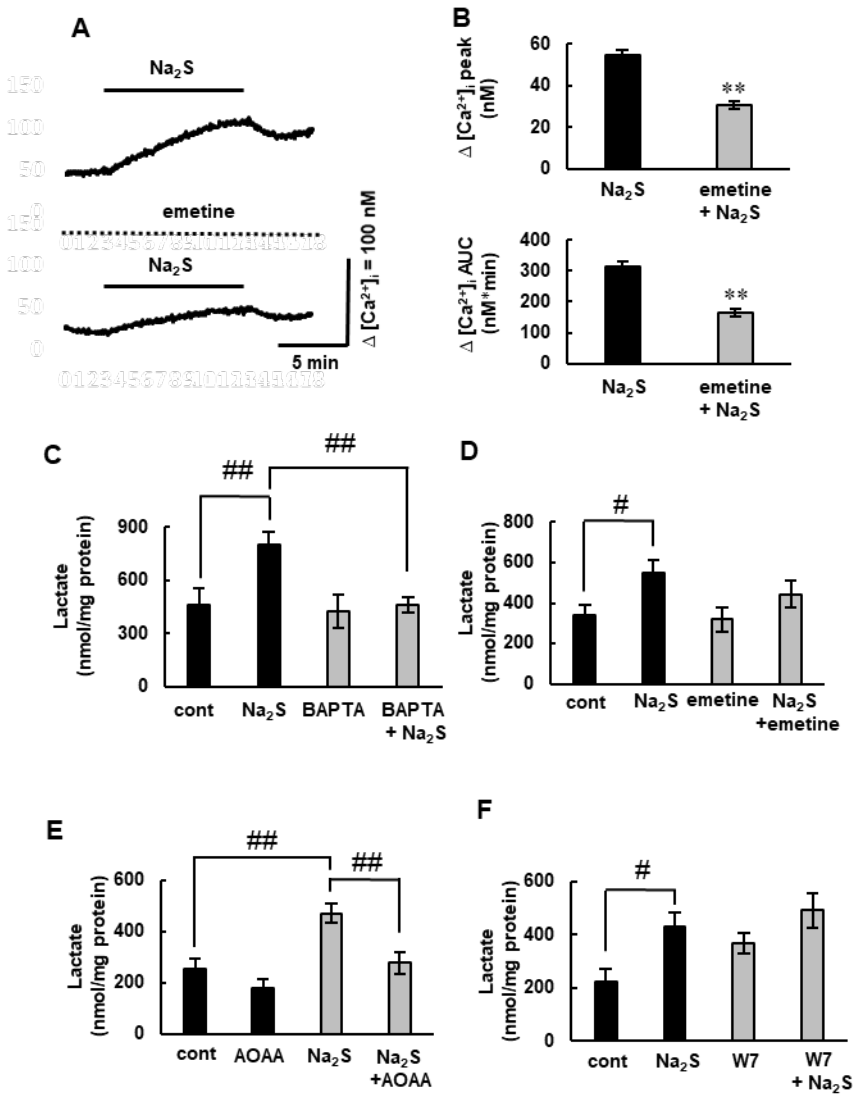
A
Na2S
emetine
Na2S
Δ [Ca2+]i = 100 nM
5 min
B
Δ [Ca2+]i peak (nM)
60
40
20
0
**
Na2S
emetine + Na2S
Δ [Ca2+]i AUC (nM*min)
400
300
200
100
0
**
Na2S
emetine + Na2S
C
Lactate (nmol/mg protein)
900
600
300
0
##
##
cont
Na2S
BAPTA
BAPTA + Na2S
D
Lactate (nmol/mg protein)
800
600
400
200
0
#
cont
Na2S
emetine
Na2S +emetine
E
Lactate (nmol/mg protein)
600
400
200
0
##
##
cont
AOAA
Na2S
Na2S +AOAA
F
Lactate (nmol/mg protein)
600
400
200
0
#
cont
Na2S
W7
W7 + Na2S